Mechanical rejuvenation and over-aging in the soft glassy rheology model

Mya Warren* and Jörg Rottler

Department of Physics and Astronomy, The University of British Columbia,
6224 Agricultural Road, Vancouver, BC, V6T 1Z1, Canada
(Dated: July 4, 2008)

Mechanical rejuvenation and over-aging of glasses is investigated through stochastic simulations of the soft glassy rheology (SGR) model. Strain- and stress-controlled deformation cycles for a wide range of loading conditions are analyzed and compared to molecular dynamics simulations of a model polymer glass. Results indicate that deformation causes predominantly rejuvenation, whereas over-aging occurs only at very low temperature, small strains, and for high initial energy states. Although the creep compliance in the SGR model exhibits full aging independent of applied load, large stresses in the nonlinear creep regime cause configurational changes leading to rejuvenation of the relaxation time spectrum probed after a stress cycle. During recovery, however, the rejuvenated state rapidly returns to the original aging trajectory due to collective relaxations of the internal strain.

PACS numbers: 81.05.Kf,83.50.-v,61.43.-j

I. INTRODUCTION

The mechanical properties of glassy materials continuously evolve due to slow, non-equilibrium dynamics, a phenomenon called physical aging [1, 2, 3]. As a consequence, the response of glasses to an applied load depends not only on measurement time, but also on the wait time t_w that has elapsed since the glass was formed. In general, increasing wait time makes glasses less compliant and increases their resistance to plastic flow [2, 3, 4, 5, 6, 7, 8, 9, 10, 11, 12, 13, 14]. For glasses formed through a rapid quench from the liquid state, the effects of aging take a particularly simple form: response functions such as the creep compliance obey a self similar scaling with the wait time and depend only on the ratio of t/t_w^μ. The aging exponent μ has been found to be approximately unity for a wide class of structural glasses moderately below the glass transition temperature [2, 15].

However, large mechanical deformation and plastic yielding can modify the aging dynamics. A primary example of this phenomenon is the observed reduction in the aging exponent obtained through creep measurements of glassy polymers at large stress. Since the relaxation times of the deformed glass resemble those of a younger glass, it was hypothesized that the glass had been "rejuvenated" by the stress [2]. Experiments on a wide variety of materials including polymer glasses [6, 16, 17], colloidal glasses [4, 5], and even the cytoskeleton of the cell [18] have shown a similar decrease in relaxation times under high loads. However, the interpretation of these results in terms of rejuvenation remains controversial. Detailed experiments by McKenna have shown that the time to equilibration of mechanically rejuvenated glasses remains essentially unchanged by the application of external load [7], suggesting that stress does not in fact change the extent of aging. Other studies indicate that the apparent enhancement of particle mobility eventually disappears after unloading [6, 17], and that the configurational states of mechanically rejuvenated glasses are distinct from the states visited by aging in the absence of load [10, 12, 19].

Signatures of over-aging due to deformation have recently been observed as well. For instance, polymer glasses subject to a stress relaxation experiment well below the glass transition temperature exhibit rapid densification for certain strains [20]. Molecular simulations of simple structural glasses show that a small amplitude strain cycle at zero temperature can decrease the inherent structure energy [10]. Also, detailed experiments by Lequeux and co-workers show over-aging in systems of dense colloids, which are effectively athermal glasses. They observe changes to the entire spectrum of relaxation times [8, 9]: after a period of small amplitude oscillatory shear, the glass appears rejuvenated over small timescales, and over-aged over longer timescales.

The emerging picture of the phenomenology of glasses under load presents some interesting questions that seem to defy a simple explanation in terms of the rejuvenation hypothesis. Firstly, under what loading conditions do over-aging and rejuvenation occur? So far, over-aging has been seen only under very specific circumstances: low temperature, small strains, and strain-controlled loading conditions. Rejuvenation, on the other hand, has been observed much more generally in deformed samples, but has been studied most extensively at high temperatures (only moderately below the glass transition temperature) and constant stress conditions. Another important question is presented by the work of McKenna [7]. What is the nature of the states created by loading, and how do we reconcile the rejuvenated relaxation spectrum with the fact that the time to equilibration is unchanged by the stress?

A comprehensive molecular model that describes aging and deformation in glasses is not available to date. However, phenomenological energy landscape approaches such as the soft glassy rheology (SGR) model [21] have

*Electronic address: mya@phas.ubc.ca

been able to capture many aspects of the rheology of glasses, and have successfully been used to interpret over-aging in strain-controlled experiments at low temperature [9, 19]. In this study, we will use the SGR model to systematically explore the loading phase diagram in order to better understand the generality and the implications of mechanical rejuvenation and over-aging, as well as the relationship between configurational and dynamical changes. We perform stochastic simulations of the SGR model over a wide range of experimental conditions and compare the results to molecular dynamics simulations of a model polymer glass in selected cases.

II. MODELS

A. Soft Glassy Rheology Model

It has been found experimentally and through molecular simulations that the structural relaxation events which result in aging and plastic deformation involve the cooperative motion of groups of approximately 10-30 particles [22, 23, 24]. The premise of the SGR model is that each of these mesoscopic rearranging domains can be described by a single fictive particle in a rough free-energy landscape. This particle performs thermally or mechanically activated hops between locally harmonic "traps" in the landscape. The density of states of the traps is

$$\rho(E) = \frac{1}{x_g} \exp(-E/x_g), \qquad E \geq 0 \qquad (1)$$

where x_g is the glass transition temperature, and E is the depth of a trap. At low temperature, many traps will be very long lived. The master equation governing the dynamics of the fictive particles is [21]

$$\begin{aligned}\dot{P}(E,l,t) &= -\dot{\gamma}\frac{\partial P}{\partial l} - P\Gamma_0 \exp\left[-\left(E - \frac{kl^2}{2}\right)/x\right] \\ &+ \Gamma(t)\rho(E)\delta(l).\end{aligned} \qquad (2)$$

$P(E,l,t)$ is the occupation probability of a state with energy E and local strain l at time t. The energy barrier for particle hopping is reduced by the local strain energy, $E_b = E - kl^2/2$ where k is the stiffness of the well. All of the barriers have a common energy of zero, so the energy of the fictive particle in the trap is $-E_b$. On the right hand side of eq. (2), the first term describes the elastic motion of the fictive particles in their wells under a strain rate of $\dot{\gamma}$. In the absence of particle hopping, this term simply increases the local strain variable of the particles. The second term in eq. (2) describes activated hopping out of the wells, which can be viewed as a local plastic yield event; Γ_0 is the attempt rate and x is a "noise temperature" [21]. The noise temperature is generally higher than the thermodynamic temperature, as it incorporates the effect of non-equilibrium fluctuations in the aging glass. The third term describes the transition to the new state after hopping, whose energy is chosen randomly from the density of states $\rho(E)$ and is initially unstrained; $\Gamma(t)$ is the total hopping rate at time t. The macroscopic stress in this formulation is

$$\sigma = k\langle l \rangle. \qquad (3)$$

We solved the master equation (2) numerically using Monte Carlo simulations of ten thousand particles under various thermo-mechanical conditions. In this work, x_g, Γ_0, and k are chosen to be one, which has the effect of setting the units of energy, time, and strain. Note that a strain of one in these units is the yield strain of an average particle. An initial configuration was created from the liquid state at $x_l > 1$ from the corresponding Boltzmann distribution and was then quenched instantaneously to the glass phase at $x < 1$. In the absence of load, the system falls out of equilibrium and exhibits full aging, i.e. an aging exponent $\mu = 1$ [25].

For the strain-controlled loading protocol, each fictive particle is treated independently. The strain variable is increased at constant rate, and at each time step the particles i hop with probability $P_i = \Gamma_i dt$ where $\Gamma_i = \Gamma_0 \exp\left[-\left(E_i - kl_i^2/2\right)/x\right]$ is the hopping rate of the particle. The stress is computed from Eq. (3), where the average is taken over all 10,000 particles. The stress-controlled loading protocol is somewhat more complicated because of the implicit relationship between the master equation and the stress. In this case, we use the kinetic Monte Carlo method [26] to evolve an ensemble of particles. A time step is chosen from a Poisson distribution with the global rate $\Gamma = \sum \Gamma_i$, and the particle that will hop is chosen with a probability proportional to each particle's individual hopping rate. The relaxed particle hops into a zero strain state, and the stress it was holding is redistributed uniformly among the particles in the system, i.e. the microscopic strains are increased evenly until Eq. (3) is satisfied again. If the stress is applied quickly, the strain energy may exceed the barrier for some elements. These are relaxed instantaneously and the procedure is repeated until a stable configuration is found.

B. Molecular Dynamics

For qualitative comparison with a structural glass, we perform molecular dynamics (MD) simulations on a "bead-spring" polymer model [27] that has been studied extensively for its glass-forming properties. In this model, beads interact via a non-specific van der Waals potential (Lennard-Jones), and bonds are modeled as a stiff spring (FENE) that prevents chain crossing. The reference length-scale is a, the diameter of the bead; the energy scale, u_0, is determined by the strength of the van der Waals potential, and the time scale is $\tau_{LJ} = \sqrt{ma^2/u_0}$, where m is the mass of a bead. The pressure and stress are therefore measured in units of u_0/a^3.

In these simulations, we consider 855 chains of 100 beads each in an originally cubic simulation volume with

periodic boundary conditions. The polymers are first equilibrated at a melt temperature of $1.2u_0/k_B$, and then quenched into the glassy state by decreasing the temperature at constant rate to below the glass transition temperature $T_g \approx 0.35u_0/k_B$ [28]. Deformation experiments are then performed on the glass at constant temperature by either applying a uniaxial load, or by imposing volume-conserving, uniaxial deformation at constant strain rate. This polymer model has been used frequently in studies of deformation of polymer glasses [29]. In particular, it demonstrates mechanical rejuvenation during nonlinear creep under large loads [14]. Except at very large strains where polymer entanglements become important, we expect these results to be pertinent for most glassy materials.

III. RESULTS

We begin exploring the loading phase diagram in the limit of zero noise temperature and zero strain rate, where over-aging has most commonly been observed. Starting configurations are created from different melt temperatures x_l. At $x = 0$, the samples are strained at constant rate to a maximum strain γ_{max} and then returned to zero strain at the same rate. The stress and the mean energy are plotted versus strain in Fig. 1 for two different initial melt temperatures. Initially, the stress is linear in strain as the system responds elastically, and then becomes constant after yield. Note that the yield stress is higher for the state that was quenched from the lower melt temperature. Also, the energy of the higher x_l configuration is lowered by the strain cycle (over-aging), whereas the lower x_l configuration has a higher energy after the same cycle (rejuvenation). These results are qualitatively similar to molecular simulation results of a binary Lennard-Jones glass at zero temperature reported in ref. [10] and appear to be generic to rough energy landscapes with many metastable states [19].

In Fig. 2, we explore in detail the effects of the noise temperature x, the initial configuration temperature x_l, and the strain rate $\dot{\gamma}$ in the strain controlled protocol described above. Here we treat x as a free adjustable parameter, although in the SGR model it is envisioned to be related to the dissipated energy of yielding elements. For each thermo-mechanical history, we compare the final energy after the strain cycle E_f to the energy E_0 of the same sample if it had not been strained, but simply aged at constant temperature for an equivalent amount of time. The relative energy difference $\Delta E/E_0$ is positive for rejuvenation, and negative for over-aging.

In Fig. 2(a) the energy difference $\Delta E/E_0$ is plotted for samples with the same x_l and $\dot{\gamma}$, but various noise temperatures x. We see that over-aging does indeed occur only at low noise temperatures, which may be why it has mostly been observed in low temperature simulations and in colloids. The small x curves show a transition from over-aging at low strains to rejuvenation at
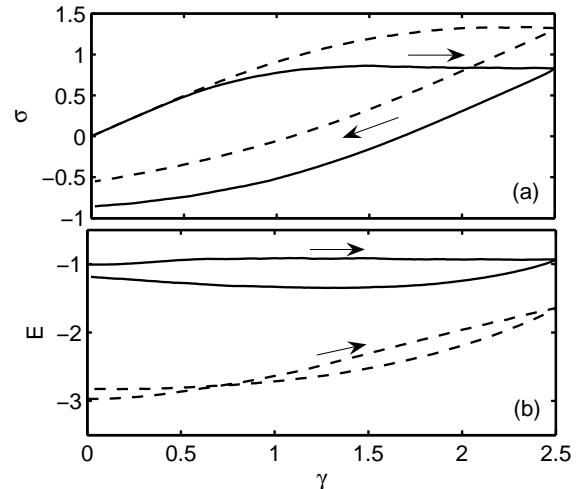

FIG. 1: (a) Stress vs. strain and (b) Energy vs. strain at zero noise temperature. The solid line is for an initial configuration at a liquid temperature of $x_l = 2$, and the dashed line corresponds to $x_l = 1.5$.
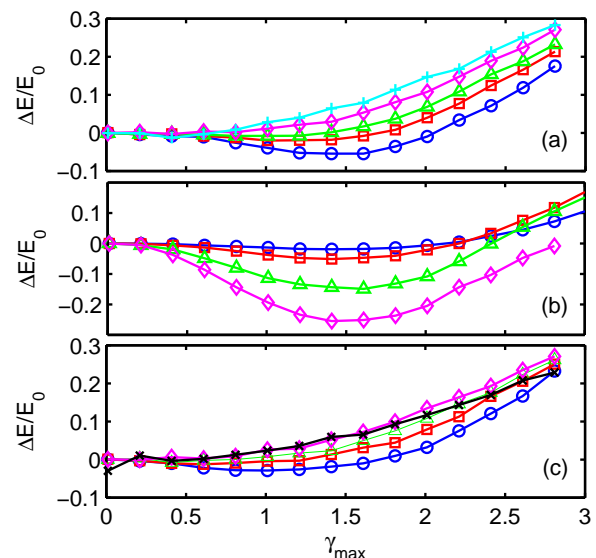

FIG. 2: (Color online) Relative difference in energy versus maximum strain after a single strain cycle of amplitude γ_{max}. (a) Noise temperature $x = 0.1$, 0.2, 0.3, 0.5, and 0.8 from bottom to top, $x_l = 2$ and $\dot{\gamma} = 0.25$ for each sample. (b) $x_l = 1.25$, 1.5, 2.5, and 5 from top to bottom, $x = 0.001$ and $\dot{\gamma} = 0.25$ for each sample. (c) $\dot{\gamma} = 1$ (circle), 0.5 (square), 0.25 (triangle), 0.1 (diamond), and 0.01 (cross), $x = 0.5$ and $x_l = 2$.

high strains. At very high strains (not shown) the glass yields, and all of the samples are maximally rejuvenated. As the noise temperature is increased, the magnitude of over-aging and the maximum strain where it occurs both decrease. For $x > 1$, the SGR model is in equilibrium and the effects of over-aging and rejuvenation disappear
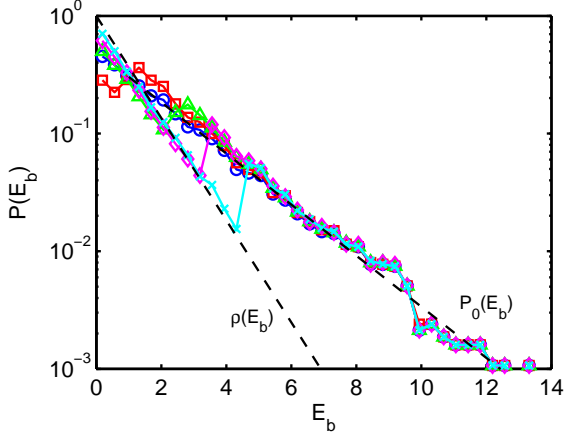
FIG. 3: (Color online) Distribution of energy barriers after a zero temperature strain cycle. γ_{max} goes from zero (dark blue circles) to 3 (light blue ×'s). The initial energy distribution $P_0(E)$ and the landscape density of states $\rho(E)$ are shown as dashed lines.
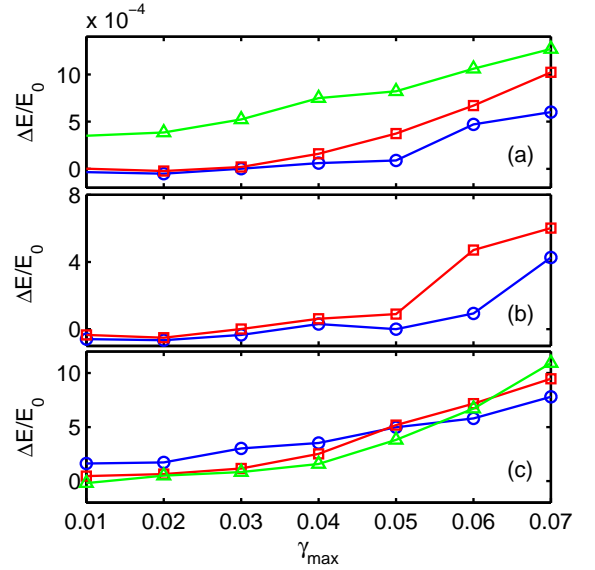

FIG. 4: (Color online) Molecular dynamics results for the relative difference in energy versus strain after a single strain cycle. (a) $T = 0.01$ (circle), 0.1 (square), and $0.2u_0/k_B$ (triangle). The quench time is $t_{qu} = 750\tau_{LJ}$ and $\dot{\gamma} = 5.3 \times 10^{-5}\tau_{LJ}^{-1}$ for each sample. (b) $t_{qu} = 750\tau_{LJ}$ (square) and $7500\tau_{LJ}$ (circle). $T = 0.01u_0/k_B$ and $\dot{\gamma} = 5.3 \times 10^{-5}\tau_{LJ}^{-1}$. (c) $\dot{\gamma} = 5.3 \times 10^{-6}\tau_{LJ}^{-1}$ (circle), $5.3 \times 10^{-5}\tau_{LJ}^{-1}$ (square), and $5.3 \times 10^{-4}\tau_{LJ}^{-1}$ (triangle). $T = 0.2u_0/k_B$, and $t_{qu} = 750\tau_{LJ}$.

except for weak transients.

Figure 2(b) shows the energy difference at very low x for various initial states x_l. The amount of over-aging decreases as the initial energy is decreased, and asymptotically approaches zero in the case of a quench from exactly $x_l = x_g$. Note that the strain at which over-aging is maximized does not seem to depend on the initial configuration, but always occurs at $\gamma_{max} \approx 1.4$. Alternatively, at higher temperatures where rejuvenation is predominant, we find that the amount of rejuvenation increases with melt temperature x_l.

Finally, the mechanical rate also plays a role in whether the energy will be reduced or increased by the strain cycle. Figure 2(c) shows relative energy changes for a sample with noise temperature $x = 0.5$ for various strain rates. The amount of rejuvenation decreases with increasing strain rate for moderate strains, but the curves eventually cross as the strain approaches yield. This is due to the fact that the yield stress (or strain) increases with rate. At the highest strain rates, over-aging appears possible even at high temperatures. Note, however, that high strain rates are not treated entirely realistically in this model. In the SGR model, an element yields instantaneously when strained to greater than the yield strain. However, in real solids, very fast strain rates lead to large affine displacements but relatively few plastic events as these require a finite time to relax.

With the SGR model, further intuition can be gained by investigating the effect of mechanical deformation on the population of the traps directly. Figure 3 shows the distribution of energy barriers for various γ_{max} after a zero noise temperature strain cycle. The strain cycle causes particles in the lowest energy states to hop into new states chosen from the landscape energy distribution $\rho(E)$. Over-aging then occurs when the states being relaxed are of lower energy than the mean energy

of the states they hop into. At zero noise temperature, this predicts that maximum over-aging occurs at a strain amplitude γ_{max} where $k\gamma_{max}^2/2 = \int_0^\infty dE\rho(E)E = 1$, or $\gamma_{max} = \sqrt{2}$. This can be seen clearly in Fig. 2(b) for all values of x_l. The strain amplitude at maximum over-aging thus gives a measure of the mean energy of the landscape. The amount of over-aging, or the energy at this peak strain, is due to the number of low energy states available to relax, and therefore depends sensitively on the initial configuration.

This picture also helps us understand why over-aging occurs primarily at low temperatures. At higher noise temperature, the low energy states that are relaxed by small strains to produce over-aging are rapidly depleted via thermal activation, meaning that the peak over-aging is drastically reduced. Additionally, thermal aging results in the relaxation of higher energy states during the strain cycle, and these states are left with residual strain energy after the cycle. Consequently, the final stress increases with noise temperature, and the effective aging during the cycle is reduced.

We compare these results with molecular dynamics simulations of the model polymer glass under similar thermo-mechanical histories by varying the maximum strain, the strain rate, and the temperature of the glass. In order to investigate the effect of different initial states, an equilibrated melt at $T = 1.2u_0/k_B$ is quenched at different rates to the final glassy temperature. The results are shown in Fig. 4 and are qualitatively similar to
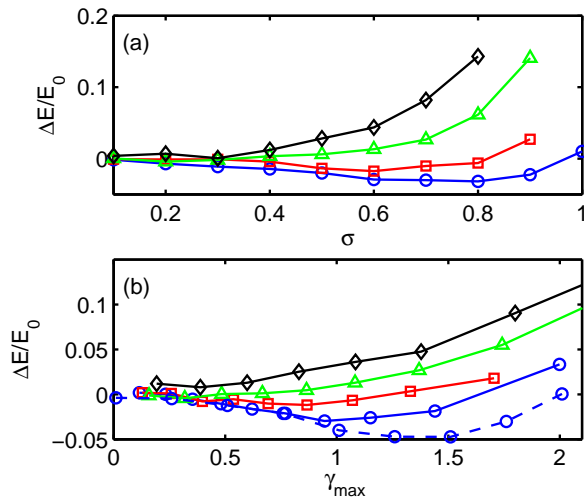
FIG. 5: (Color online) Relative energy change due to a stress cycle applied for $t = 10$. In (a) the energy difference is plotted versus the stress, and in (b) the same data is plotted versus the maximum strain in the stress cycle. $x = 0.1$ (circles), 0.2 (squares), 0.4 (triangles), and 0.6 (diamonds). $x_l = 2$ for each sample. The dashed line in (b) is the energy versus strain for an equivalent strain-controlled protocol at $x = 0.1$.

behaviour found in the SGR model. Figure 4(a) shows that higher temperatures lead to increased rejuvenation, Fig. 4(b) shows that initial states of higher energy (faster quench) result in more rejuvenation, and Fig. 4(c) shows increased rejuvenation at moderate strains as well as decreased rejuvenation at large strains as the strain rate is decreased. However, there is a significant difference between the SGR and molecular dynamics results. We have not found appreciable over-aging in our molecular dynamics simulations, even at very low temperatures and fast cooling rates. This is in contrast to recent molecular dynamics results of an atomistic polymer model under a similar strain cycle [12]. The authors of this study report over-aging of the simulated glass by the strain for very fast quench rates. However, this is likely because they did not compare to a non-strained control sample but to the initial (just quenched) energy before the strain cycle. We observe that even at very low temperatures, our model exhibits significant aging directly after the glass is quenched when quench rates are very high. It remains an open question to what extent over-aging occurs in real polymer glasses under realistic quench and loading conditions.

Stress-controlled loading protocols similarly show rejuvenation and over-aging in the SGR model. In this case, a stress step function is applied for a period of $t = 10$ and then released. The change in energy due to the stress cycle is plotted in Fig. 5(a) for various noise temperatures. At low noise temperature, there is over-aging at low stress and rejuvenation at high stress. At high noise temperature, there is a broad flat region for small stress, followed by a steep increase in rejuvenation at high stress
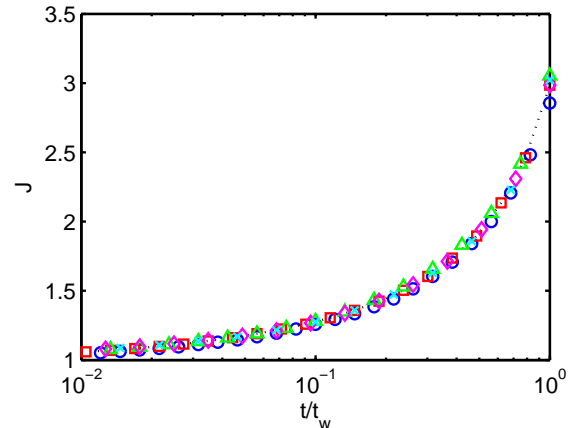

FIG. 6: (Color online) Creep compliance of the SGR model quenched from $x_l = \infty$ (see text) and aged for $t_w = 100$ (circles), 316 (squares), 1000 (triangles), 3162 (diamonds), and 10000 (×'s) at $x = 0.5$ and $\sigma = 0.75$ (within the nonlinear regime).

within the nonlinear regime. In Fig. 5(b), the same data is plotted versus the maximum strain achieved during the stress cycle for direct comparison with the strain-controlled data. The results plotted in this way look very similar to Fig. 2(a) for the strain cycle. Over-aging occurs over a similar range of noise temperature and strain, however, closer inspection shows that the amount of over-aging is somewhat smaller for the stress-controlled protocol. Finishing the cycle at zero stress rather than zero strain means that low energy states that did not relax during the experiment have residual strain energy and are rejuvenated.

Our analysis so far has utilized changes in the energy of the system to identify the occurrence of rejuvenation or over-aging. However, the notion of rejuvenation has its origin in an acceleration of the dynamics under load [2, 4, 5, 6, 7, 8]. As described earlier, rejuvenation is commonly measured via a decrease in the aging exponent μ with applied stress σ. Experimentally, the aging exponent can be evaluated through creep experiments: superposition of the creep compliance $J(t, t_w)$ of samples that have aged for different wait times t_w reveals the t/t_w^μ scaling behaviour. In principle, this type of analysis can also be performed in the SGR model, but is impeded by the fact that the creep compliance exhibits a clear t/t_w scaling only in the limit of $t_w \to \infty$ [30]. In particular, for quenches from a finite liquid temperature x_l, we find that the scaling regime is not accessible within a reasonable simulation time. In the creep experiments described below, we therefore initialize the trap distribution from $\rho(E)$, where the scaling regime is more easily accessible. This is equivalent to performing a quench from $x_l = \infty$. Figure 6 shows representative compliance curves for several different wait times under an applied load of $\sigma = 0.75$. Indeed, compliance curves obey the t/t_w scaling behaviour characteristic of trap models
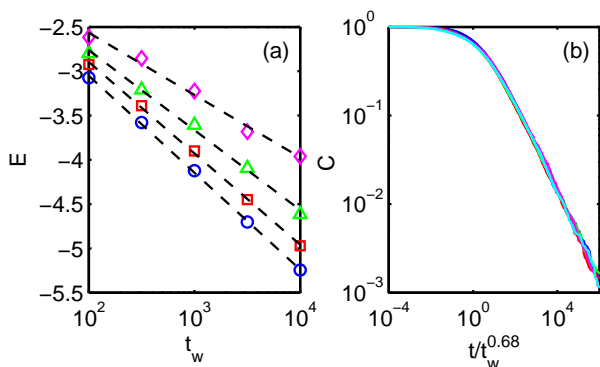
FIG. 7: (Color online) (a) Energy as a function of wait time after a stress cycle of duration $t = t_w$. $\sigma = 0.05$ (circles), 0.6 (squares), 0.7 (triangles), 0.75 (diamonds). $x = 0.5$ and $x_l = \infty$ for each sample. (b) Scaled correlation functions for $t_w = 100$, 316, 1000, 3162, and 10000 (all overlapping) for $\sigma = 0.75$. Data collapse is obtained for $\mu = 0.68$.
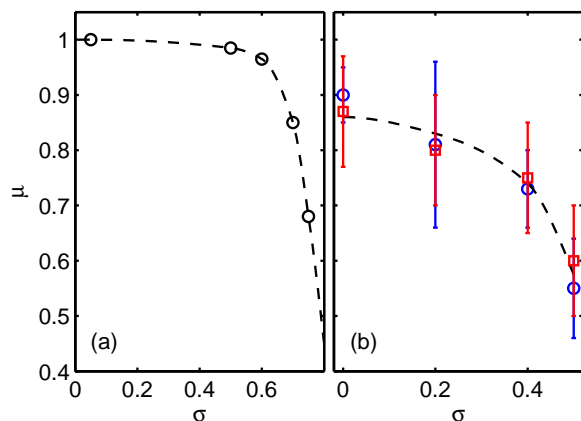

FIG. 8: (Color online) (a) Aging exponent versus the stress in the SGR model, as determined from the correlation functions eq. (4) after a stress cycle of duration $t = t_w$. $x = 0.5$ and $x_l = \infty$. (b) Aging exponent versus stress from molecular dynamics simulations of a model polymer glass using (circles) the creep compliance and (squares) the mean-squared displacement after stress release at $10t_w$. $T = 0.2u_0/k_B$.

[25]. Interestingly, we find this scaling behaviour to be independent of the magnitude of the applied stress, even within the nonlinear creep regime. Although the form of the scaling function is stress dependent [30], the decrease in the aging exponent under large load that is observed in real structural glasses does not occur in the SGR model.

However, it is clear from the data in Fig. 5 that large stress cycles cause rejuvenation of the energy of the ensemble. To test the effect of wait time on the state of the aged samples after creep, we release the stress after a creep experiment of duration t_w and measure the average energy of the unloaded system. Figure 7(a) plots the energy vs wait time for four different stresses and shows that not only does the energy change nonlinearly with

the stress as anticipated from Fig. 5, but the slope of the energy versus wait time curves also decreases for increasing stress. Highly stressed samples appear to have aged less.

The simple relationship between the energy and the dynamics in the SGR model implies a simultaneous change in the dynamics after the stress is released. To see this, we compute the correlation function

$$C(t, t_w) = \int_0^\infty dE_b P(E_b, t, t_w) e^{-\left(\Gamma_0 e^{-E_b/x}\right)t} \quad (4)$$

which measures the probability that a particle in a trap at time t_w has not hopped at time $t_w + t$ [25]. These functions are shown in Fig. 7(b) for various wait times after a nonlinear stress cycle. The shape of the correlation function is typical of glasses, although missing the initial β-relaxation decay. There is a plateau region at short times where there are very few relaxation events, followed by a rapid decrease at $t \approx t_w$. In contrast to the compliance curves, the scaling of correlation functions with t_w after the cycle is drastically changed by large stresses. Figure 7(b) shows that for $\sigma = 0.75$, the correlation functions no longer display full aging behavior, but we find good data collapse if we rescale time with t_w^μ, where $\mu = 0.68$. It appears that for stress controlled deformation at finite temperature, the relaxation time spectrum of the mechanically rejuvenated glass does indeed resemble a younger glass.

Figure 8(a) presents the variation of aging exponents with stress obtained from superposition of the correlation functions at different wait times. At small stresses, the exponent is unity, but decreases rapidly for nonlinear creep. For comparison with the polymer model, we repeat the creep experiment using molecular dynamics following a similar protocol. In MD, we extract aging exponents from superposition of mean squared displacements (see ref. [14]) of particles after stress release. Figure 8(b) shows that these exponents (squares) similarly decrease with increasing stress amplitude. Remarkably, aging exponents obtained by superposition of creep compliance curves (circles) appear to be identical to those found through mean-squared displacements after the stress is released. This indicates that the change in the aging exponent observed in nonlinear creep experiments is due to the evolving configuration of the glass, rather than the direct effect of stress on energy barriers, which would cease when the stress is removed.

It seems that the SGR model does produce rejuvenation in the relaxation times, but is the mechanically rejuvenated glass actually taken back in time by the application of stress? If this were the case, we would expect the relaxation after stress to proceed exactly like the younger, unstressed glass. In Fig. 9, we investigate the recovery of a glass after a stress cycle and compare to the natural aging trajectory of an unstressed glass. We see that the aging progresses much more rapidly after the stress cycle, and asymptotically approaches the energy relaxation of the unstressed sample. This is the essence of the paradox
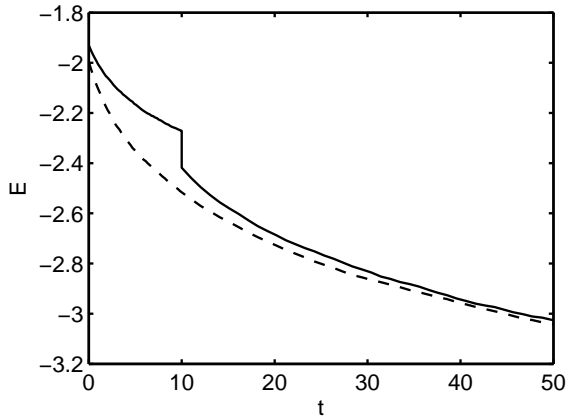
FIG. 9: Energy during a stress cycle and the subsequent recovery (solid line) compared to an unstressed glass (dashed). Here $x = 0.75$, $x_l = 2$ and $\sigma = 0.5$.

pointed out by McKenna [7]: although the stressed glass has an apparently rejuvenated relaxation spectrum, the time it takes to reach equilibrium is unchanged. In the SGR model, this has a simple explanation. Every time a trap relaxes, it releases the strain it was holding. Therefore, at constant (zero) stress, each relaxation causes a decrease in the strain energy of the entire ensemble of particles. This leads to a return to the unstrained aging trajectory over a timescale similar to the decay of the correlation function. It is conceivable that in real glasses, interactions between relaxing elements similarly explain McKenna's observations.

IV. CONCLUSIONS

We have performed stochastic simulations of the SGR model for strain-controlled and stress-controlled loading cycles in the glassy phase. Both types of loading induce changes to the mean energy of the glass corresponding to regimes of mechanical rejuvenation and over-aging. Within the SGR model, rejuvenation is the predominant effect, while over-aging is only observed at low strains, low temperatures, and high energy initial configurations. These results are in qualitative agreement with molecular dynamics simulations of a model polymer glass over a wide range of loading parameters.

In addition to changes in the energy of the glass, mechanical rejuvenation is often observed as a decrease in the aging dynamics. To this end, we have evaluated the aging exponent through the scaling of the creep compliance with wait time, in direct analogy with experiment. As previously remarked in ref. [30], the creep compliance in the SGR model strictly obeys full aging ($\mu = 1$), even at very high load. In contrast, experiments [2, 4, 16] and MD simulations [14] show that the aging exponent decreases with stress amplitude in the nonlinear creep regime. The physics of this phenomenon does not seem to be captured by the SGR model; instead, the dynamical effects of mechanical rejuvenation appear only after the stress cycle. Aging exponents found from the t_w scaling of correlation functions after unloading decrease with increased stress, in qualitative agreement with MD simulations. Reconciling the stress dependence of the aging exponent in the SGR model with experiment would be a fruitful topic for further development of the model, but may require a better understanding of the physics of mechanical rejuvenation at the molecular level.

Finally, we have explored the relaxation dynamics after a rejuvenating stress cycle. The SGR model exhibits the fundamental difficulty with the "rejuvenation" hypothesis. While the relaxation times after a stress cycle appear to be exactly identical to a younger glass, when the stress is released, the aging trajectory gradually returns to the undeformed path [7]. In the SGR model, this effect is due to collective strain relaxation which occurs after each hopping event. Identifying the effects of structural relaxations on the rejuvenated state may similarly provide insight to this effect in real glasses.

[1] C. A. Angell, K. L. Ngai, G. B. McKenna, P. F. McMillan, and S. W. Martin, J. Applied Physics **88**, 3113 (2000).
[2] L. C. E. Struik, *Physical Aging in Amorphous Polymers and Other Materials* (Elsevier, Amsterdam, 1978).
[3] J. M. Hutchinson, Prog. Polym. Sci. **20**, 703 (1995).
[4] M. Cloitre, R. Borrega, and L. Leibler, Phys. Rev. Lett. **85**, 4819 (2000).
[5] D. Bonn, S. Tanase, B. Abou, H. Tanaka, and J. Meunier, Phys. Rev. Lett. **89**, 015701 (2002).
[6] J. J. Martinez-Vega, H. Trumel, and J. L. Gacougnolle, Polymer **43**, 4979 (2002).
[7] G. B. McKenna, J. Phys.: Condens. Matter **15**, S737 (2003).
[8] V. Viasnoff and F. Lequeux, Phys. Rev. Lett. **89**, 065701 (2002).
[9] H. Montes, V. Viasnoff, S. Juring, and F. Lequeux, Faraday Discuss. **123**, 253 (2003).
[10] D. J. Lacks and M. J. Osborne, Phys. Rev. Lett. **93**, 255501 (2004).
[11] M. Utz, P. G. Debenedetti, and F. H. Stillinger, Phys. Rev. Lett. **84**, 1471 (2000).
[12] A. V. Lyulin and M. A. J. Michels, Phys. Rev. Lett. **99**, 085504 (2007).
[13] J. Rottler and M. O. Robbins, Phys. Rev. Lett. **95**, 225504 (2005).
[14] M. Warren and J. Rottler, Phys. Rev. E **76**, 031802 (2007).
[15] K. Chen and K. S. Schweizer, Phys. Rev. Lett. **98**, 167802 (2007).

[16] A. Lee and G. B. McKenna, Polymer **31**, 423 (1990).

[17] H.-N. Lee, K. Paeng, S. F. Swallen, and M. D. Ediger, J. Chem. Phys **128**, 134902 (2008).

[18] P. Bursac, G. Lenormand, B. Fabry, M. Oliver, D. A. Weitz, V. Viasnoff, J. P. Butler, and J. J. Fredberg, Nature Materials **4**, 557 (2005).

[19] B. A. Isner and D. J. Lacks, Phys. Rev. Lett. **96**, 025506 (2006).

[20] D. M. Colucci, P. A. O'Connell, and G. B. McKenna, Polym. Eng. Sci. **37**, 1469 (1997).

[21] P. Sollich, F. Lequeux, P. Hebraud, and M. E. Cates, Phys. Rev. Lett. **78**, 2020 (1997).

[22] R. E. Courtland and E. R. Weeks, J. Phys.:Condens. Matter **15**, S359 (2003).

[23] K. Vollmayr-Lee and E. A. Baker, Europhysics Lett. **76**, 1130 (2006).

[24] P. Schall, D. A. Weitz, and F. Spaepen, Science **318**, 1895 (2007).

[25] C. Monthus and J. P. Bouchaud, J. Phys. A: Math. Gen. **29**, 3847 (1996).

[26] A. B. Bortz, M. H. Kalos, and J. L. Lebowitz, J. Comp. Phys. **17**, 10 (1975).

[27] K. Kremer and G. S. Grest, J. Chem. Phys **92**, 5057 (1990).

[28] J. Rottler and M. O. Robbins, Phys. Rev. E **64**, 051801 (2001).

[29] R. A. Riggleman, K. S. Schweizer, and J. J. de Pablo, Macromolecules (in press) (2008).

[30] S. M. Fielding, P. Sollich, and M. E. Cates, J. Rheology **44**, 329 (2000).